Measurement Parameters Optimized for Sequential Multilateration in Calibrating a Machine Tool with a DOE Method

Fabien Ezedine, Jean-Marc Linares, Julien Chaves-Jacob, Jean-Michel Sprauel

applied sciences

MDPI

Article

Measurement Parameters Optimized for Sequential Multilateration in Calibrating a Machine Tool with a DOE Method

Fabien Ezedine, Jean-Marc Linares *, Julien Chaves-Jacob and Jean-Michel Sprauel

Institute Movement Science, CNRS, ISM, Aix Marseille University, Marseille 13009, France; ezedinefabien@gmail.com (F.E.); julien.chaves-jacob@univ-amu.fr (J.C.-J.); jean-michel.sprauel@univ-amu.fr (J.-M.S.)

* Correspondence: jean-marc.linares@univ-amu.fr ; Tel.: +33-442-939-096

Academic Editor: Kuang-Cha Fan

Received: 15 September 2016; Accepted: 14 October 2016; Published: 25 October 2016

Abstract: Improving volumetric error compensation is one of the machine tool user's key objectives. Smart compensation is bound to calibration accuracy. Calibration quality depends largely on its setup factors. An evaluation criterion is thus required to test the quality of the compensation deduced from these setup factors. The residual error map, which characterizes post-compensation machine errors, is therefore chosen and then needs to be evaluated. In this study, the translation axes of a machine tool were calibrated with a multilateration tracking laser interferometer. In order to optimize such measurements, the residual error map was then characterized by two appliances: a laser interferometer and the tracking laser already employed for the calibration, using for that purpose the sequential multilateration technique. This research work thus aimed to obtain a smart setup of parameters of machine tool calibration analyzing these two residual error maps through the Design Of Experiment (DOE) method. To achieve this goal, the first step was to define the setup parameters for calibrating a compact machine tool with a multilateration tracking laser. The second step was to define both of the measurement processes that are employed to estimate the residual error map. The third step was to obtain the optimized setup parameters using the DOE method.

Keywords: machine tool; calibration; compensation; tracking laser; sequential multilateration; error map

1. Introduction

Over the two last decades, the economic situation has imposed new constraints in terms of quality, productivity, cost, and production time. These constraints evolved faster than machine tool performances. Accordingly, there has been a need to improve machine tool efficiency. The objective has been to match machine tool capability with the geometrical requirements of manufactured parts. The lack of accuracy observed in workpieces is due to several systematic machine errors: kinematic and thermally induced effects are the major contributors. The source of the kinematic errors are mainly machine tool part geometry and misalignment of the different guideways and rotary axis [1,2]. In the workshop, the direct environment of a machine tool can significantly influence the thermal behavior of its structure [3]. Internal heat sources such as the drive motors, the electronic and pneumatic systems, the spindle, and the linear guides induce gradients of temperature that imply the expansion of machine tool parts [4–7]. Load and cutting strength are non-negligible effects to consider, too [8,9]. One way to improve the volumetric accuracy of a machine tool is to enhance machine tool design. However, expenses incurred and physical and technological limitations restrict this implementation. It is economically more viable to estimate and then adapt to these errors using numerical compensation. As soon as the error is systematic and repeatable, the pre-calibrated error compensation is effective.

The aim is to numerically change tool trajectory to minimize the locating error between the real tool trajectory and the ideal toolpath. Several techniques and appliances are used to estimate this error in the whole discretized working volume: telescopic ball-bar [10,11], 3D probe-ball [12], R-test [13], laser technology [14–16], etc. Laser techniques are the most widespread appliances in the research field and the tracking laser is the most reliable instrument used [15,16]. Its advantages are the submicron measurement resolution and the high number of data that may be collected. Afterwards, the computed compensation matrix is combined with a mathematical model based on the machine structure to generate a compensated toolpath. For this purpose, homogenous transformation matrices are widely used [17,18]. Improving volumetric error compensation is one of the machine tool users' key objectives. Smart compensation is bound to calibration accuracy. Calibration quality depends largely on its setup factors. An evaluation criterion is thus required to test the quality of the compensation deduced from these setup factors. The residual error map, which characterizes post-compensation machine error, is therefore chosen and then needs to be evaluated. The appliance used for the evaluation usually has to be different from the one used to determine the calibration. In this study, the translation axes of a five-axis machine tool are calibrated with a multilateration tracking laser (TL). The residual error map is then characterized by two different appliances: a classical laser interferometer (LI) and the TL already used for the calibration.

This research work aimed to provide optimized setup parameters for machine tool calibration using a design of experiment (DOE) method. To achieve this objective, the first step was to present the setup parameters for calibrating a compact five-axis Computer Numerical Control (CNC) machine tool with a TL. The second step was to define the measurement processes employed with both instruments (TL and LI) to estimate the residual error map. The third step was to introduce the methodology applied to obtain optimized setup parameters. A DOE was used for that purpose. Finally, the results obtained with the two appliances were compared, and the best practice for implementing machine tool calibration is here proposed.

2. Calibration Setup Parameters of Multilateration Method

The setup parameters that influence the calibration can be stated in three different categories that depend on their origin: the machine tool, the TL, and the measuring environment. These sources are shown in Table 1. For each source, the studied parameters (designation, unit and value) are defined. Among these parameters, some are fixed while others are to be optimized. These setup parameters are described here in after.

Table 1. Setup parameters.

Source	Parameter	Unit	Value
Machine tool	Warming cycle	-	Yes
	Plate material	-	Steel
	Feedrate	mm/min	1000
Tracking laser	Type of pattern	-	Box
	Sampling step	mm	10
	Acquisition time	s	**Optimized**
	Number of offsets	-	4
	Offset size	mm	**Optimized**
	Number of TL positions	-	**Optimized**
Environment	Room temperature	°C	20

2.1. Machine Tool Setup Parameters

As mentioned above, kinematic errors are significantly sensitive to thermally induced effects. To avoid the thermal expansion of its structure, the studied machine tool was customized. Three different cooling systems controlled the temperature of the numerical controller card, the drive motors, and the spindle (DMG MORI, Roissy, France). Moreover, a set of thermal probes (ETALON,

Braunschweig, Germany) was placed on the machine tool and used to compensate the thermal drift of the linear guides. Before starting the measurement, a warming cycle was applied to ensure that the thermal expansion of these guides is stabilized. This warming up of the linear axes of the machine tool consisted of a CNC program by simultaneously moving the three axes of the machine. The toolpaths can cover the entire working volume of the studied machine. The feed rate of the three axes was set to 5000 mm/min. The thermal sensors (ETALON, Braunschweig, Germany) placed near the axes allowed for the monitoring of the temperatures until thermal stabilization of the mechanical structure. Preheating time lasted about 20 mins before the beginning of the measurements. Due to the excessive weight of the TL, this appliance was bound to the machine bed via a self-made support plate which was also subject to thermal expansions. As the machine was mainly composed of steel, the same material was used for it. Finally, a compromise concerning the feedrate had to be made between the limitation of the dynamic effects of the machine tool and the calibration time. A rate of 1000 mm/min is a wise choice in that it minimizes these two constraints.

2.2. Tracking Laser Setup Parameters

In this study, a TL system was used [1]. Its distinctive characteristic is that it can accurately estimate the distance between a reference sphere bound to the appliance and another sphere (the reflector) attached to a mobile item. The form defect of these two spheres and the evolution of their position are the major factors that deteriorate length measurement. To minimize these parasitic effects, the form defect of the reference sphere was less than 50 nm, and an invar support avoids any displacement of the reference sphere due to thermal expansion. Temperature and air pressure were also recorded and used by the acquisition software (V2.3, ETALON, Braunschweig, Germany) to compensate laser beam deviation. The TL characterized the distance between the two spheres. At least four length measurements in four different TL locations were then required to determine the reflector position. This principle, shown in Figure 1, is called multilateration. TL*j*, where j = 1 to 4, is the position of the TL reference spheres, and I1 is the reflector location.

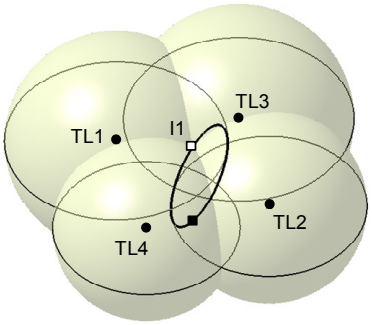

Figure 1. Multilateration principle.

The use of four TLs is quite expensive, and few laboratories or companies can afford such investment. However, the reflector location can be determined using only one appliance, by simply shifting its position three times. This is called sequential multilateration. It is the method used in this study.

Sequential multilateration is the main source of factors that influence machine tool calibration. The kind of pattern, which defines machine tool trajectory geometry, needs to be characterized. It leans on the outlines of the compact working volume (box pattern: 200 × 200 × 280 mm) as shown in Figure 2. The linear guide kinematic errors are greater at the start and end positions, which constitute the most critical cases. The distance between the two consecutive nodes (sampling step) of the box edges needs to be fixed. Ten millimeters is an acceptable distance to correctly sample the box pattern (Figure 2). Moreover, the dynamic variation of the machine tool engenders some reflector oscillations. Once the machine tool stops, the TL carries out a sampling of the distances measured during a predetermined

acquisition time. The distance estimated is the mean of the sampled values. The acquisition time is a parameter taken into account in the optimization process.

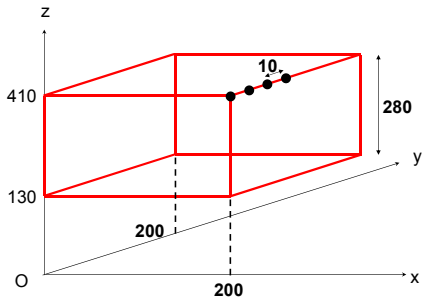

Figure 2. Box pattern.

The location of the measurement appliances also strongly influences calibration quality [19]. The reflector (ETALON, Braunschweig, Germany) needs to be equally spread around the spindle axis. Machine tool compactedness makes this operation difficult to implement as shown in Figure 3. A fixing system was designed to place the reflector in different locations without reducing the working area of the machine tool. This self-made fixing system uses a metal strap. It surrounds the spindle of the machine tool and supports the reflector. The mechanical part has cylindrical bores that allows the reflector to be in different orientations and positions using a set of rods and connectors. In this study, the number of reflector locations was limited to four. An overly large offset size puts the reflector outside the working volume during measurement and may engender some collision with the machine tool bed. According to Abbe's principle, the offset size amplifies the locating errors that are easier to estimate. It then needs to be optimized. Spreading the TL positions around the working volume is a factor to consider. In this study, machine tool compactedness made it necessary to position the TL in front of the machine tool. Figure 4 shows two different positions. As a consequence, this parameter had to be optimized. The minimum number of TL positions imposed by the multilateration technique is four.

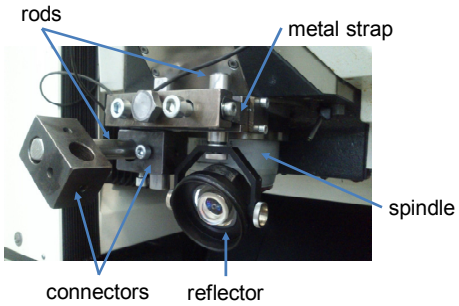

Figure 3. Fixing system of the reflector around the spindle.

Figure 4. Two tracking laser (TL) positions.

2.3. Environment Setup Parameters

As mentioned previously, the internal heat sources are controlled. The thermal effects of external heat sources have to be limited too. For that purpose, an air conditioner system regulates the temperature in the machine tool room (20 °C ± 1 °C).

To summarize this section, the three setup parameters allocated for the optimization process are the number of TL positions, the reflector offset size, and the acquisition time. The optimization of these three parameters using the DOE process is detailed in Section 4. The next section introduces the criterion used to evaluate the quality of the compensation.

3. Machine Tool Compensation Assessment

Three steps are required to estimate the residual error map: the calibration process, the compensation process, and compensation assessment. Figure 5 summarizes the complete experimental procedure. Each step is described in the following subsections.

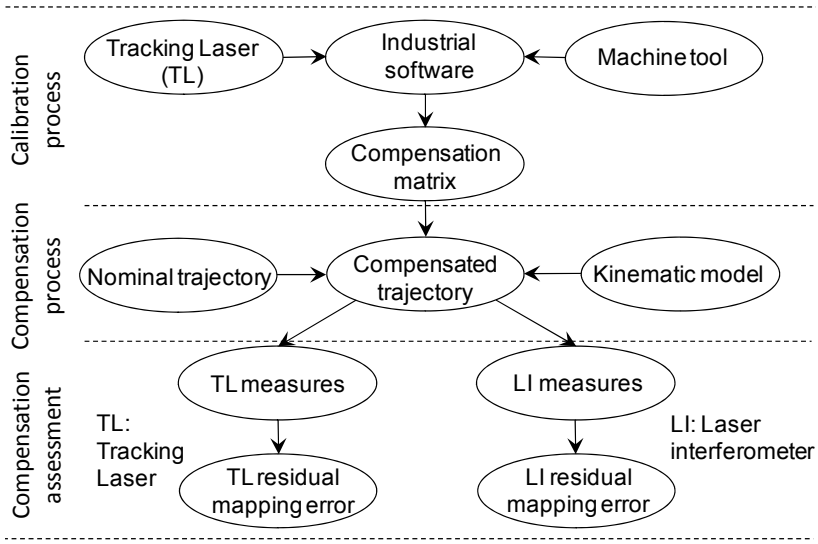

Figure 5. Residual error maps estimation.

3.1. Calibration Process

The first step consists in calibrating the machine tool. The machine tool drives the reflector following the trajectory defined by the box edges. The compensation matrix derived from the measures carried by the TL is provided by the industrial software of the instrument. It states the kinematic errors of the machine tool at each node of the 3D mesh of the working volume.

3.2. Compensation Process

The second step is the compensation process. This operation is carried out with a Visual Basic Application macro. It consists in correcting the nominal trajectory (set of P points) with the error vector $\mathbf{d_p}$ to obtain the compensated trajectory (set of C points, with $\mathbf{OC} = \mathbf{OP} + \mathbf{d_p}$). This vector is derived from B-spline interpolations of the 18 kinematic errors and the three squareness errors of the compensation matrix, and the nominal coordinates of the trajectory point P. For that purpose, the kinematic model of the bridge-type machine tool, as shown in Figure 6, is required. S and P respectively refer to the reference point of the spindle and to the cutting edge location.

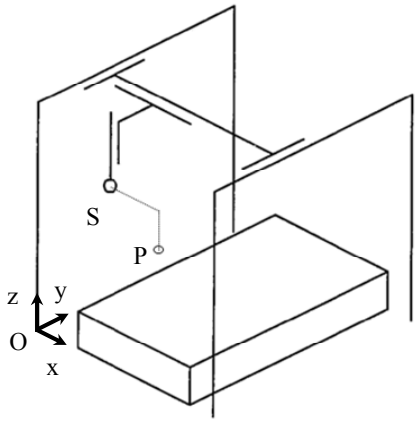

Figure 6. Structure of the studied linear axes.

In general, a homogenous transformation matrix is used to define the kinematic errors of a given translation axis. The machine tool structure is considered as rigid, which implies that the kinematic errors are proper to the node and independent from the other axes. Two types of errors exist: linear and angular. The linear drifts are characterized by a positioning error and two straightness errors. The angular errors are roll, pitch, and yaw motion errors. For an x-axis motion for example, the matrix terms are respectively noted δ_{xx}, δ_{xy}, δ_{xz}, ε_{xx}, ε_{xy} and ε_{xz}. The homogenous transformation matrix, used to compute the kinematic error for a x-axis motion, is given in Equation (1). The squareness errors of the axis system (x, y, z) of the machine are written α_s, β_s and γ_s.

$$\begin{bmatrix} 1 & -\varepsilon_{xz} & \varepsilon_{xy} & \delta_{xx} \\ \varepsilon_{xz} & 1 & -\varepsilon_{xx} & \delta_{xy} \\ -\varepsilon_{xy} & \varepsilon_{xx} & 1 & \delta_{xz} \\ 0 & 0 & 0 & 1 \end{bmatrix}. \tag{1}$$

A global transformation matrix that describes the machine tool locating error is determined. It accounts for the kinematic chain of the mechanical links and the 21 parameters of the machine kinematical error: six concerning each axis (x, y and z) and the three squareness errors of the reference frame. Then, the error vector $\mathbf{d_p}$ can be written at any point S that belongs to the spindle. Spindle rotation is not taken into account. Equation (2) defines the error vector at the cutting edge point P. The two homogeneous transformation matrices $\mathbf{A}$ and $\mathbf{A_p}$ respectively define the effects of the 21 error components on the locating error of the machine structure and the angular errors of the spindle.

$$\mathbf{d_P} = \mathbf{A}.\mathbf{OS} + \mathbf{A_P}.\mathbf{SP} \tag{2}$$

$$\mathbf{A} = \begin{pmatrix} 0 & -\gamma_s & \varepsilon_{yy} + \varepsilon_{xy} + \beta_s & \delta_{xx} + \delta_{yx} + \delta_{zx} \\ \varepsilon_{yz} & 0 & -(\varepsilon_{yx} + \varepsilon_{xx} + \alpha_s) & \delta_{xy} + \delta_{yy} + \delta_{zy} \\ -\varepsilon_{yy} & 0 & 0 & \delta_{xz} + \delta_{yz} + \delta_{zz} \\ 0 & 0 & 0 & 1 \end{pmatrix};$$

$$\mathbf{A_P} = \begin{pmatrix} 0 & -(\varepsilon_{xz} + \varepsilon_{yz} + \varepsilon_{zz}) & \varepsilon_{xy} + \varepsilon_{yy} + \varepsilon_{zy} & 0 \\ \varepsilon_{xz} + \varepsilon_{yz} + \varepsilon_{zz} & 0 & -(\varepsilon_{xx} + \varepsilon_{yx} + \varepsilon_{zx}) & 0 \\ -(\varepsilon_{xy} + \varepsilon_{yy} + \varepsilon_{zy}) & \varepsilon_{xx} + \varepsilon_{yx} + \varepsilon_{zx} & 0 & 0 \\ 0 & 0 & 0 & 1 \end{pmatrix}.$$

3.3. Compensation Assessment

The TL and the LI are used to evaluate the applied compensation. For this purpose, a residual error map is estimated by each appliance.

3.3.1. Laser Interferometer Measurements

The LI is one of the appliances used to estimate the residual error map of the machine tool. Then, fewer linear trajectories are defined in the whole working volume, which is discretized, as a 3D mesh as shown in Figure 7.

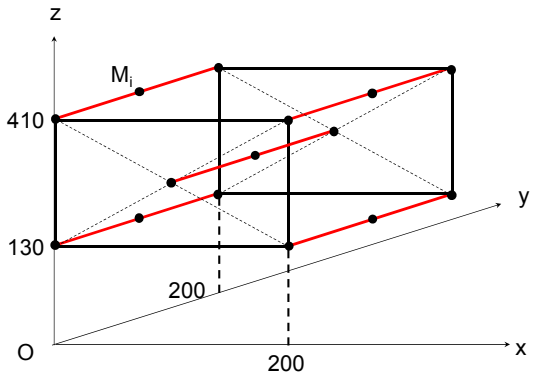

Figure 7. Laser interferometer (LI) measurement.

Once the different elements of the LI are aligned, the positioning error and the vertical and horizontal straightness are measured three times for each of the N points of the trajectory, even if the repeatability of the appliance is acceptable. These length data are used to evaluate the components of the error vector. For that purpose, different optics are used and the ISO 230-2 standard provides the experimental protocol to measure the errors of the linear axes. Due to the dead-zone, counter initialization at the first node of the line is required. Once the error vector of all the nodes is estimated, the residual error map is computed. The norm of each error vector is then calculated, and its mean value is finally defined. Equation (3) shows the norm of the error vector (re_i), where pe_i, sv_i and sh_i respectively refer to the positioning error and the vertical and horizontal straightness values measured at the point M_i ($1 \leq i \leq N$) of the compensated trajectory.

$$re_i = \sqrt{{pe_i}^2 + {sv_i}^2 + {sh_i}^2}. \tag{3}$$

The weakness of this method is the misalignment between the y-axis and the LI axis. This source of experimental error is called the cosine error. A best fit process is implemented to correct this misalignment. As a consequence, the error vector is truncated but its behavior remains unchanged.

3.3.2. Sequential Multilateration Measurement Using a TL

From an experimental point of view, data acquisition is easier with the TL than with the LI. The measurement process is faster but data analysis is more complex. The coordinates in the machine tool reference frame of N points M_i (x_i, y_i, z_i), with i = 1 to N, are estimated using the multilateration technique. For this purpose, a set of four lengths L_{ij} is defined for each point M_i, corresponding to four positions j of the TL. Equation (4) defines the mathematical relationship between the measured length L_{ij}, the coordinates of the different TL positions, the four respective dead-zones (DZ_j) and the coordinates of the points M_i. TL_j (x_{TLj}, y_{TLj}, z_{TLj}) is the TL location for position j.

$$e_{ij} = L_{ij} + DZ_j - \sqrt{\left(x_i - x_{TLj}\right)^2 + \left(y_i - y_{TLj}\right)^2 + \left(z_i - z_{TLj}\right)^2}. \tag{4}$$

Then, a non-linear least squares method is used to determine the four TL positions and the four respective dead-zones. This consists in minimizing the sum of all $4.N$ squared errors e_{ij}. Afterwards, the set of coordinates of the points M_i (x_i, y_i, z_i) is estimated. The residual error vector $\mathbf{PM_i}$ is thus

computed where P is the nominal coordinates of the cutting edge. Finally, the mean of all the error vector norms is deduced.

In this section, the residual error map was estimated by each measurement appliance (LI and TL). To estimate the quality of the calibration process, the mean value of all the error vector norms is used as a quality meter. This is called the mean residual error. In the following section, this parameter will be named Y_1 for the results obtained with the LI and Y_2 for the experiments carried out with the TL. This is the data that was used to analyze the two sets of setup calibration parameters. The following section explains how the response surface of a DOE was used to achieve this aim.

4. Optimization of the Calibration Setup Parameters

This section details the entire DOE method used to compare the two optimized setup parameters deduced from the two residual error maps. It consists in providing a mathematical model of the mean residual error (the responses Y_1 and Y_2) in function of the three influential parameters mentioned above. To do so, a sequence of experiments that mixes pre-determined values of parameters is carried out. The two appliances are able to provide the mean residual error for each experiment. These are the two responses Y_1 and Y_2 of the DOE, respectively obtained with the LI and the TL. A quadratic approximation of the response surfaces is used in the DOE. It is expressed by Equation (5), where k refers to the number of the response (1 or 2).

$$Y_k = \mathbf{B}_k.\mathbf{X} = b_{0k} + b_{1k}.X_1 + b_{2k}.X_2 + b_{3k}.X_3 + b_{12k}.X_1.X_2 + b_{13k}.X_1.X_3 + b_{23k}.X_2.X_3 + b_{11k}.X_1^2 + b_{22k}.X_2^2 + b_{33k}.X_3^2 \quad (5)$$

The reduced centered and normalized factors X_m (m = 1 to 3) represent the calibration setup parameters. These factors are noted as follows: X_1 = acquisition time, X_2 = the number of TL positions, and X_3 = the reflector offset size. $\mathbf{B_k}$ is vector of the coefficients that is used to quantify the direct and combined effects of the factors on the response k.

A composite matrix is used to determine the DOE sequence of experiments. The sequence is randomized to minimize experimental bias. The index of the experiment is noted l and ranges between 1 and 18. The matrix of experiments is shown in Table 2. The central experiment (0, 0, 0) was repeated 4 times to quantify the experimental repeatability. Three normalized levels are used for each factor: −1, 0 and +1. The real values of the setup parameters are shown in Table 3.

Table 2. Experimental plan.

Experiments	X_1	X_2	X_3
1	−1	−1	−1
2	1	−1	−1
3	−1	1	−1
4	1	1	−1
5	−1	−1	1
6	1	−1	1
7	−1	1	1
8	1	−1	−1
9	−1	0	0
10	1	0	0
11	0	−1	0
12	0	1	0
13	0	0	−1
14	0	0	−1
15	0	0	0
16	0	0	0
17	0	0	0
18	0	0	0

Table 3. Factors used in the design of experiment (DOE) process.

Factors	DOE			
	Notation	**Lower Value**	**Middle Value**	**Upper Value**
Acquisition time (s)	X_1	0.5	1	1.5
Number of TL positions	X_2	4	5	6
Offset size	X_3	Small	Medium	Large

The response surfaces are defined by a least squares optimization, and their associated statistical confidence boundaries (SCBs) are computed and plotted. The SCB is the theoretical surface envelop derived from the covariance matrix of the set of coefficients b, as deduced from the least squares residues, and calculated for a given risk α. In this study, 5% is the value chosen for α, which is commonly accepted in the metrological field. This leads to a coverage factor s that is rounded to two. As already pointed out, the best estimators $\hat{\mathbf{B}}_k$ of the two sets of experimental responses Y_k are determined by a least squares optimization, using the pseudo inverse method. Subsequently, the error bars $U(\hat{Y}_k)$ of the estimated responses $\hat{Y}_k$ are determined. They are derived from the least squares residues. Their computation is shown in Equation (6). For that purpose, the standard deviations σ_{Ek} are deduced as shown by Equation (7). N_e and N_f respectively represent the number of experiments and the number of factors. For each response, Y_k and any experiment l, the residue E_{lk} is computed and its standard deviation σ_{Ek} is then derived. Afterwards, σ_{Ek} is propagated to obtain the variance–covariance matrix of $\hat{\mathbf{B}}_k$ ($\mathbf{var}\hat{\mathbf{B}}_k$). Finally, the Jacobian of the quadratic models is used to propagate the variance-covariance matrices of $\hat{\mathbf{B}}_k$ to obtain the error bars $U(\hat{Y}_k)$, shown in Equation (8). The SCB surfaces are plotted using the set of error bars $U(\hat{Y}_k)$.

$$E_k = Y_k - \hat{\mathbf{B}}_k.\mathbf{X}; \tag{6}$$

$$\sigma_{Ek} = \sqrt{\frac{1}{N_e - N_f}.\sum_{l=1}^{N_e} E_{lk}^2}; \tag{7}$$

$$U(\hat{Y}_k) = s.\sqrt{\mathbf{J}.\mathbf{varB_k}.\mathbf{J}^{\mathrm{T}}}, \text{with } s = 2. \tag{8}$$

The two sets of optimized setup parameters can finally be determined. For that purpose, X_{mopt} (m = 1 to 3) are obtained by minimizing the responses as shown by Equation (9):

$$Y_{\mathrm{kopt}} = \min_{Xm}(\hat{Y}_k). \tag{9}$$

5. Discussion

Figure 8 shows the mean residual errors Y_1 and Y_2 for the entire sequence of experiments. The plotted point named "WC" corresponds to a measurement carried out without compensation. It characterizes the mean machine tool error existing without compensation.

The values recorded by the LI and the TL respectively turn at around 8 and 3 µm. The TL measures are of the same order as the data provided by the machine tool manufacturer. Figure 8 highlights the relative similarity between the two sets of measures. The two sets of values are vertically shifted. As explained in Section 3.3.1, this is because the LI measurement truncates the real error vector. Table 4 shows the entire set of estimated parameters derived from the coefficient matrix $\hat{\mathbf{B}}_k$ (k = 1 and 2).

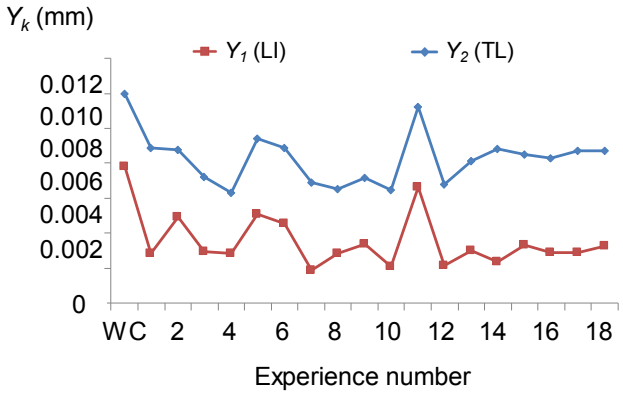

Figure 8. Set of responses Y_1 and Y_2.

Table 4. Estimated coefficients for $\hat{Y}_1$ and $\hat{Y}_2$ quadratic models.

Coefficient	$\hat{Y}_1$	$\hat{Y}_2$
$\hat{b}_0$	2.77×10^{-3}	8.44×10^{-3}
$\hat{b}_1$	1.17×10^{-4}	-2.63×10^{-4}
$\hat{b}_2$	-8.68×10^{-4}	-1.35×10^{-4}
$\hat{b}_3$	-7.02×10^{-4}	1.21×10^{-4}
$\hat{b}_{11}$	-1.29×10^{-4}	-1.48×10^{-4}
$\hat{b}_{22}$	1.23×10^{-3}	7.17×10^{-4}
$\hat{b}_{33}$	-6.15×10^{-4}	1.43×10^{-4}
$\hat{b}_{12}$	-4.38×10^{-4}	-7.29×10^{-5}
$\hat{b}_{13}$	1.43×10^{-4}	1.45×10^{-4}
$\hat{b}_{23}$	-1.89×10^{-4}	-9.5×10^{-4}

To ease the comparison between the two quadratic models, a Student test (*t*-test) is applied to the set of coefficients $\hat{\mathbf{B}}_1$ and $\hat{\mathbf{B}}_2$ characterizing $\hat{Y}_1$ and $\hat{Y}_2$ to simplify the expressions of the response surfaces. Only the factors that significantly influence the response are kept. The result is summarized in Equations (10) and (11).

$$\hat{Y}_1 = (\hat{b}_0)_1 + (\hat{b}_1)_1 \cdot X_1 + (\hat{b}_{12})_1 \cdot X_1 \cdot X_2 + (\hat{b}_{11})_1 \cdot X_1^2 + (\hat{b}_{22})_1 \cdot X_2^2; \quad (10)$$

$$\hat{Y}_2 = (\hat{b}_0)_2 + (\hat{b}_1)_2 \cdot X_1 + (\hat{b}_{12})_2 \cdot X_1 \cdot X_2 + (\hat{b}_{11})_2 \cdot X_1^2 + (\hat{b}_{22})_2 \cdot X_2^2. \quad (11)$$

The two models are not identical, but similar. In the case of a compact machine tool, the offset size X_3 does not significantly influence the residual error map. Whatever the appliance used, only the acquisition time X_1 and the number X_2 of the TL positions matter in calibrating a machine tool using a TL. Therefore, the response surfaces, which represent $\hat{Y}_1$ and $\hat{Y}_2$, are plotted only in function of X_1 and X_2. The two responses and their respective SCBs are presented through a 3D graph, which is shown in Figure 9.

The order of magnitude of the error bars computed respectively for $\hat{Y}_1$ and $\hat{Y}_2$ are 2 and 0.8 µm. The lower value estimated for the results obtained with the TL is explained by more reliable measurements and data acquisition processes. The TL is, therefore, the appliance better able to check the calibration that it provided. Nevertheless, the two sets of optimized setup parameters are identical. On the other hand, since the residual error map provided by the LI is truncated, only the response $\hat{Y}_2$ is used to provide the optimized calibration setup factors. The results are summarized in Table 5.

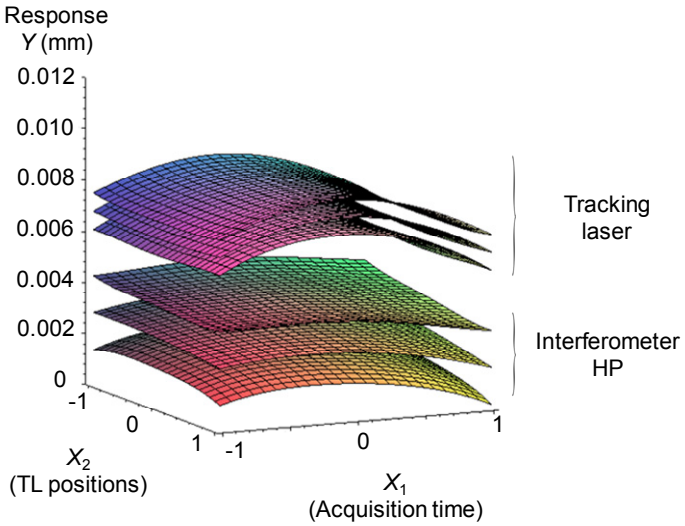

Figure 9. $\hat{Y}_1$ and $\hat{Y}_2$ response surfaces.

Table 5. Results of the DOE optimization.

X_{1opt}	X_{2opt}	Y_{opt} (µm)	Y_{wc} (µm)
1.5	6	5.99	12.2

The optimized acquisition time is 1.5 s. At any time the machine reaches a node, and a measure is carried out by the TL, the reflector takes time to stabilize. A total of 1.5 s is the time necessary to obtain a stable reflector position and a good estimation of the distance between the two spheres of the TL. The second advantage is to enable calibration using the sequential multilateration technique within half a day. In the DOE study, the number of TL positions varied between four and six. Six is the optimum value obtained with the optimization process. This is explained by the strong asymmetry of the TL positions around the working volume.

6. Conclusions

The optimization of machine tool calibration method optimization has been a key objective for two decades in the manufacturing field. Multilateration using TL is one of the most important assets to achieve this aim. Calibration quality depends largely on its setup factors. An evaluation criterion is required to test the quality of the compensation deduced from the setup factors. A residual error map, which characterizes post-compensation machine error, is thus chosen and then needs to be evaluated. The appliance used for the evaluation usually has to be different from the one used to determine the calibration (independence between the calibration phase and the quality compensation verification phase). In this paper, two instruments were therefore used to estimate the residual error map: a classical laser interferometer (LI) and a tracking laser (TL). The multilateration technique was applied in the second case. The result obtained by the multilateration TL delivered a complete 3D error map. On the other hand, an error vector was also characterized by a classical interferometer laser. It was, however, limited to the projection of each real error vector onto the measurement direction, thus truncating the residual error. The TL using the multilateration method turned out to be the best solution to estimate the residual error existing after compensation. Based on these two residual error estimations, the sets of machine tool calibration setup factors were optimized using design of experiment (DOE) methodology. The same optimal setup parameters were derived from the results obtained with both the classical interferometer and the multilateration tracking laser, which, however, provided the lowest uncertainty. Considering the studied experimental range, the length of the offset between the TL and the machine tool cutting edge appeared as an insignificant setup parameter. In the

case of calibration of a compact machine tool, it is preferable to minimize it. The difficult access to the working volume implies that the TL has to be placed in front of the machine tool. As a consequence, the optimized number of TL positions was found to be six, which is the largest value considered in this study. As regards the acquisition time, the optimized value was estimated at 1.5 s to stabilize the measure. Finally, the entire set of results suggests that the TL is self-sufficient to carry out a full calibration–compensation process for a compact CNC machine tool.

Acknowledgments: The experimental devices used in this work were founded by the European Community, French Ministry of Research and Education, Pays d'Aix Conurbation Community, and Aix Marseille Université.

Author Contributions: Fabien Ezedine was responsible for the experiments. The data was analyzed by Jean-Michel Sprauel and Jean-Marc Linares. Julien Chaves-Jacob conceived and manufactured the self-made fixing devices. All the authors participated to the writing of the paper.

Conflicts of Interest: The authors declare no conflict of interest.

References

1. Schwenke, H.; Knapp, W.; Haitjema, H.; Weckenmann, A.; Schmitt, R.; Delbressine, F. Geometric error measurement and compensation of machines-an update. *CIRP Ann.-Manuf. Technol.* **2008**, *57*, 660–675. [CrossRef]
2. Díaz-Tena, E.; Ugalde, U.; De Lacalle, L.L.; De la Iglesia, A.; Calleja, A.; Campa, F.J. Propagation of assembly errors in multitasking machines by the homogenous matrix method. *Int. J. Adv. Manuf. Technol.* **2013**, *68*, 149–164. [CrossRef]
3. Mian, N.S.; Fletcher, S.; Longstaff, A.P.; Myers, A. Efficient estimation by FEA of machine tool distortion due to environmental temperature perturbations. *Precis. Eng.* **2013**, *37*, 372–379. [CrossRef]
4. Gomez-Acedo, E.; Olarra, A.; De Lacalle, L.L. A method for thermal characterization and modeling of large gantry-type machine tools. *Int. J. Adv. Manuf. Technol.* **2012**, *62*, 875–886. [CrossRef]
5. Gebhardt, M.; Mayr, J.; Furrer, N.; Widmer, T.; Weikert, S.; Knapp, W. High precision grey-box model for compensation of thermal errors on five-axis. *CIRP Ann.-Manuf. Technol.* **2014**, *63*, 509–512. [CrossRef]
6. Mayr, J.; Jedrzejewski, J.; Uhlmann, E.; Donmez, M.A.; Knapp, W.; Härtig, F.; Wendt, K.; Moriwaki, T.; Shore, P.; Schmitt, R.; et al. Thermal issues in machine tools. *CIRP Ann.-Manuf. Technol.* **2012**, *61*, 771–791. [CrossRef]
7. Donmez, M.; Blomquist, D.S.; Hocken, R.J.; Liu, C.R.; Barash, M.M. A general methodology for machine tool accuracy enhancement by error compensation. *Precis. Eng.* **1986**, *8*, 187–196. [CrossRef]
8. Archenti, A.; Nicolescu, N. Accuracy analysis of machine tools using Elastically Linked Systems. *CIRP Ann.-Manuf. Technol.* **2013**, *62*, 503–506. [CrossRef]
9. Yuan, J.; Ni, J. The real-time error compensation technique for CNC machining systems. *Mechatronics* **1998**, *8*, 359–380. [CrossRef]
10. Abbaszadeh-Mir, Y.; Mayer, J.R.R.; Cloutier, G.; Fortin, C. Theory and simulation for the identification of the link geometric errors for a five-axis machine tool using a telescoping magnetic ball-bar. *Int. J. Prod. Res.* **2002**, *40*, 4781–4797. [CrossRef]
11. Lei, W.T.; Hsu, Y.Y. Error measurement of five-axis CNC machines with 3D probe–ball. *J. Mater. Proc. Technol.* **2003**, *139*, 127–133. [CrossRef]
12. Weikert, S. R-Test, a New Device for Accuracy Measurements on Five Axis Machine Tools. *CIRP Ann.-Manuf. Technol.* **2004**, *53*, 429–432. [CrossRef]
13. Castro, H.F.F.; Burdekin, M. Calibration system based on a laser interferometer for kinematic accuracy assessment on machine tools. *Int. J. Mach. Tools Manuf.* **2006**, *46*, 89–97. [CrossRef]
14. Aguado, S.; Santolaria, J.; Samper, D.; Velázquez, J.; Javierre, C.; Fernández, Á. Adequacy of Technical and Commercial Alternatives Applied to Machine Tool Verification Using Laser Tracker. *Appl. Sci.* **2016**, *6*, 100. [CrossRef]
15. Schneider, C.T. Lasertracer—A New Type of Self Tracking Laser Interferomete. In Proceedings of the 8th International Workshop on Accelerator Alignment, Geneva, Switzerland, 4–7 October 2004.
16. Schwenke, H.; Franke, M.; Hannaford, J. Error mapping of CMMs and machine tools by a single tracking interferometer. *CIRP Ann.-Manuf. Technol.* **2005**, *54*, 475–478. [CrossRef]

17. Lei, W.T.; Sung, M.P. NURBS-based fast geometric error compensation for CNC machine tools. *Int. J. Mach. Tools Manuf.* **2008**, *48*, 307–319. [CrossRef]
18. Schwenke, H.; Schmitt, R.; Jatzkowski, P.; Warmann, C. On-the-fly calibration of linear and rotary axes of machine tools and CMMs using a tracking interferometer. *CIRP Ann.-Manuf. Technol.* **2009**, *58*, 477–480. [CrossRef]
19. Linares, J.M.; Chaves-Jacob, J.; Schwenke, H.; Longstaff, A.; Fletcher, S.; Flore, J.; Wintering, J. Impact of measurement procedure when error mapping and compensating a small CNC machine using a multilateration laser interferometer. *Precis. Eng.* **2014**, *38*, 578–588. [CrossRef]